INTERPRETATION OF ELECTRIC FIELDS IN CORONAL MAGNETIC LOOPS

P. Foukal
Atmospheric and Environmental Research, Inc., Cambridge, MA 02139
D. Landman
Institute for Astronomy, University of Hawaii, Honolulu, HI 96822

1. INTRODUCTION

Stark effect detected in high Balmer lines emitted from flares, prominences, and quiet chromosphere is generally interpreted as pressure broadening in a plasma of relatively high density. But a recent study of post-flare loops indicates that the densities of order 10^{12} cm^{-3} required to explain the observed Balmer line broadening are an order of magnitude higher than values derived using other plasma diagnostics such as Thomson scattering and Balmer line emission measures (Foukal, Miller, and Gilliam 1983). The disagreement might be explained as the difference expected between the true local density (measured by the Stark effect) in the obviously inhomogeneous loop plasma, and the straight mean or root mean square densities measured by Thomson scattering and line emission measures. More interestingly, the disagreement might imply a macroscopic electric field generated by, e.g., plasma waves in coronal magnetic loops.

The purpose of this study is to distinguish between these two interpretations using the density sensitivity of certain MgI, NaI, and SrII line intensity ratios recently calculated by Landman (1983, 1984). The lines of interest are formed at roughly the same temperatures as the Balmer lines and turn out to be quite bright in post flare loops. Since these line ratios respond to the local density in the loop condensations, comparison of the densities obtained simultaneously and co-spatially from them and from Stark effect should yield fairly direct information on possible macroscopic electric fields.

2. INSTRUMENTATION AND OBSERVING PROCEDURES

The spectra of post-flare loops analyzed here were obtained at the 40 cm coronograph and Universal spectrograph at the SPO Big Dome. Most of the spectra cover the wavelength region between approximately 3600 Å and 4500 Å in a single 10-30 sec exposure, at a dispersion of 1.6 Å/mm in third order at 3950 Å. This wavelength range includes the density sensitive line ratio MgI($\lambda\lambda 3833,3838$)/SrII($\lambda 4078$) on one frame, together with the Balmer lines of interest down to the series limit. In order to measure the two other useful line ratios calculated by Landman; MgI($\lambda\lambda 5173,5184$/SrII($\lambda 4078$) and NaI($\lambda\lambda 5890,5896$)/SrII($\lambda 4078$) the intensities of the MgI b and NaI D lines must be measured from a separate spectrum obtained several minutes later. Since pointing errors and loop evolution can lead to significant changes over this time scale, the values of density obtained from these two ratios carry less weight.

3. DATA AND REDUCTION PROCEDURE

The spectra were traced on a microdensitometer and the background (sky-scattered Fraunhofer spectrum) was subtracted. The lines were then fitted with least-squares Gaussian profiles to derive FWHM values $\Delta\lambda_{1/2}$ for the Balmer lines, and peak intensities for the relevant lines of MgI, NaI, and SrII. Fig. 1 shows the spectral regions around the MgI($\lambda\lambda3833,3838$) lines and around the SrII($\lambda4078$) line, for one of the spectra taken of a bright loop on 19 Dec. 1982. These lines were well calibrated in all our loop spectra. The calibration data required to compare I($\lambda4078$) to the MgI b and NaI D line intensities were only available for the one loop of 11 Aug. 1972, so only for that loop were we able to derive densities from all three of the ratios calculated by Landman.

4. RESULTS

a) Stark effect

Fig. 2 shows plots of the observed Balmer line halfwidths $\Delta\lambda_{1/2}$ against the upper principal quantum number n, for two of the five loops. The solid curves are quadratic fits to the data. These two loops, for which four and five spectra each are averaged, show a clear broadening beyond H 12-14, which suggests Stark effect. The dashed curves represent the values of $\Delta\lambda_{1/2}$ taken from tabulated Stark effect calculations of Kurochka (1969). These tables give total halfwidths for different values of Gaussian broadening due to thermal, microturbulent motions and instrumental function. The plotted curves provide the best fit to the minimum observed halfwidth near n = 10 and to the halfwidth increase between n ~ 10 and n ~ 20. The densities required to produce the observed broadening are in the range 1-2 x 10^{12} cm^{-3}.

Similar plots for the three other loops, for which only one spectrum each was reduced, show some evidence of a broadening of comparable slope, but at a considerably lower significance level. Only for the two loops discussed above do we have sufficient data to show that the trend of halfwidth with Balmer number is significant.

b) Line Ratios

Fig. 3 shows calculated curves of the most observationally reliable line intensity ratio I($\lambda\lambda3833,3838$)/I($\lambda4078$) against density for T_e = 5 x 10^3 K and 8 x 10^3 K, showing the range of the ratio observed in these loops and the corresponding densities. In the two loops for which several Balmer line spectra are available, the densities obtained from this intensity ratio are 1-2 x 10^{12} and > 10^{13} cm^{-3}. The densities found in the other three loops (at an equal level of significance) are much lower, between 1-3 x 10^{11} cm^{-3}.

The line-ratio densities obtained from the two ratios carrying lower weight show a large scatter, not in very good agreement with the I($\lambda\lambda3833,38$)/I($\lambda4078$) ratio densities presented above. This large internal variation is probably caused by the pointing and loop evolution errors mentioned previously.

26

5. CONCLUSIONS

The main conclusions of this study so far are:

i) The Stark effect and line intensity ratio diagnostics agree to within a factor 2 when the data of highest statistical weight are compared. They both indicate high densities of $n_e \gtrsim 10^{12}$ cm^{-3} in the cool condensations within post-flare loops. This is encouraging agreement for two plasma diagnostic techniques with quite different sources of error.

ii) These data of highest weight indicate that electric fields in post flare loops can be understood as pressure broadening expected in a dense plasma. Large scale d.c. or plasma-wave electric fields as large as 10^2 volts cm^{-1} may also be present, but they would be difficult to detect by this technique alone.

iii) The $I(\lambda\lambda 5173,5184)/I(\lambda 4078)$ and $I(\lambda\lambda 5890,5896)/I(\lambda 4078)$ ratios seem to yield lower values for the loop condensations than does the $I(\lambda\lambda 3833,3838)/I(\lambda 4078)$ ratios. This disagreement is most likely due to pointing changes and evolution of the loop condensations, since the former two ratios were not accessible on one exposure. But a larger sample of loop spectra on which at least one of the other two line ratios can be measured simultaneously would be desirable to verify the high densities recorded in the ratio $I(\lambda\lambda 3833,3838/I(\lambda 4078)$.

iv) The three loops for which the Balmer line broadening has lower weight show a Stark effect that would still require $n_e \sim 0.5$-2×10^{12} cm^{-3}, but the line ratio density yields a value of only 1-3×10^{11} cm^{-3} for these loops. One might conclude that all post-flare loops contain macroscopic E fields of order 10^2 v cm^{-1}, and only in the most dense loops does the pressure broadening produce microscopic electric fields of the same order. A larger sample of loops needs to be studied to check this possibility.

References

Foukal, P., P. Miller, and L. Gilliam, Sol. Phys., 83, 83, 1983.

Kurochka, L., Soviet Astr. (A.J.), 13, 64, 1969.

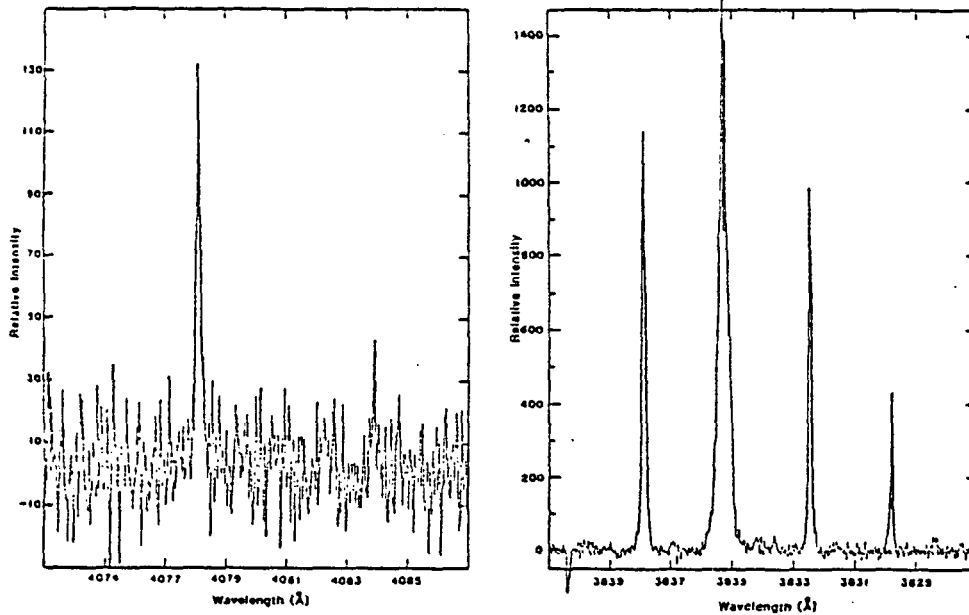Landman, D., Ap. J., 269, 728, 1983.

Landman, D., Ap. J., 279, 438, 1984.

27

Figure 1. The spectral regions around the SRII(λ4078) line (left) and MgI(λλ3833,3838) lines (right) in the spectrum of the loop observed on 19 Dec. 1982.
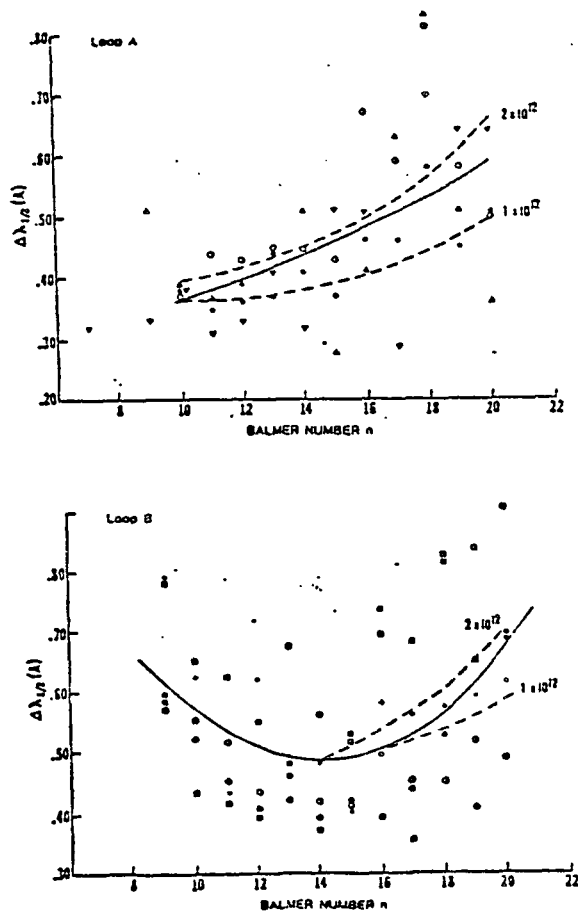

◄ Figure 2. Plots of the FWHM $\Delta\lambda_{1/2}$ of Balmer lines against upper principal quantum number n, for the two loops of highest statistical weight. See text for explanation of the dashed lines.
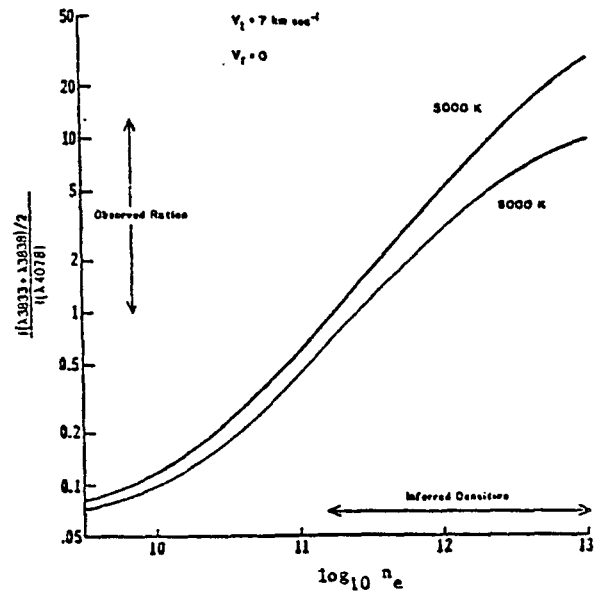

Figure 3. Plot of the MgI intensity ratio against electron density.

28